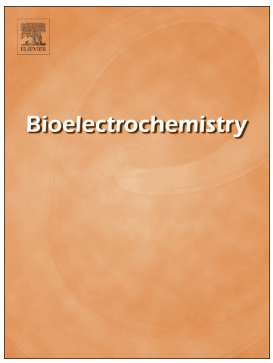

Interaction of prednisone with dsDNA at silver nanoparticles/ poly(glyoxal-bis(2-hydroxyanil))/dsDNA modified electrode and its analytical application

Gözde Aydoğdu Tığ, Derya Koyuncu Zeybek, Bülent Zeybek, Şule Pekyardımcı

PII: S1567-5394(18)30075-6
DOI: https://doi.org/10.1016/j.bioelechem.2018.11.003
Reference: BIOJEC 7216

To appear in: *Bioelectrochemistry*

Received date: 15 February 2018
Revised date: 6 November 2018
Accepted date: 6 November 2018

Please cite this article as: Gözde Aydoğdu Tığ, Derya Koyuncu Zeybek, Bülent Zeybek, Şule Pekyardımcı , Interaction of prednisone with dsDNA at silver nanoparticles/ poly(glyoxal-bis(2-hydroxyanil))/dsDNA modified electrode and its analytical application. Biojec (2018), https://doi.org/10.1016/j.bioelechem.2018.11.003

Interaction of prednisone with dsDNA at silver nanoparticles/poly(glyoxal-bis(2-hydroxyanil))/dsDNA modified electrode and its analytical application

Gözde Aydoğdu Tığ[1,*] gaydogdu@science.ankara.edu.tr, Derya Koyuncu Zeybek[2], Bülent Zeybek[3], Şule Pekyardımcı[1]

[1]Department of Chemistry, Faculty of Science, Ankara University, Ankara, Turkey

[2]Department of Biochemistry, Faculty of Arts and Science, Kütahya Dumlupınar University, Kütahya, Turkey

[3]Department of Chemistry, Faculty of Arts and Science, Kütahya Dumlupınar University, Kütahya, Turkey

[*]Corresponding author.

Abstract

This paper reports the fabrication of an electrochemical DNA biosensor for the electrochemical determination of prednisone (PRD), which is a synthetic corticosteroid. For this purpose, silver nanoparticles (AgNPs) and a new polymer film poly(glyoxal-bis(2-hydroxyanil)) (P(GBHA)) were electrochemically deposited on a glassy carbon electrode (GCE), respectively. Then, an electrochemical DNA biosensor was prepared onto this electrode surface (GCE/AgNPs/P(GBHA)) by the immobilization of dsDNA using a chronoamperometry method. The proposed electrode was characterized by FESEM, XPS, and cyclic voltammetry (CV). The interaction between the PRD and dsDNA immobilized on the GCE/AgNPs/P(GBHA) electrode was investigated via a differential pulse voltammetry (DPV) method and UV-Vis spectrophotometry. The experimental factors affecting the interaction between the PRD concentration and dsDNA were optimized. The fabricated biosensor showed a wide linear response in a PRD concentration range of 1.0−50.0 μg mL^{-1} depending on both the adenine and

guanine base signals. The detection limit based on the guanine and adenine signals was 0.3 μg mL^{-1} and 0.25 μg mL^{-1}, respectively. The sensor exhibited excellent anti-interferential ability, good stability and reproducibility and was satisfactorily employed for the electrochemical assay of PRD in serum samples. The new DNA biosensor can be utilized for the sensitive, accurate and rapid analysis of PRD.

Keywords: dsDNA, biosensor, differential pulse voltammetry, prednisone, interaction

1. Introduction

Prednisone (PRD) is a synthetic corticosteroid commonly prescribed in the treatment of a broad variety of inflammatory diseases such as asthma, rheumatoid arthritis, various kidney diseases including nephritic syndrome, allergies and cluster headache [1]. Steroids such as PRD are used to suppress the immune system and thus suppress inflammatory response. They are particularly effective in reducing the swelling and pain that accompanies inflammation [2]. Therefore, the determination of PRD is important for the treatment and progress of a variety of important diseases.

The various methods that have been reported for PRD detection include high-performance liquid chromatography [3], electrospray ionisation single quadrupole mass spectrometry [4], on-line solid-phase extraction liquid chromatography and tandem mass spectrometry [5], polarography [6] and electrochemical techniques [7, 8]. In the last decade, the development of electrochemical techniques for the analysis of PRD has increased significantly. These methods show advantages such as simple design, cost effectiveness, good stability and repeatability [9].

Recently, there has been increasing interest in the electrochemical examination of the interaction between drugs and dsDNA [10]. Electrochemical DNA biosensors include a nucleic acid recognition layer immobilized onto an electrochemical transducer. The recognition layer

determines the alterations that have formed in the DNA structure during the interaction of DNA with drug molecules [11]. Hence, the studies on the binding mode of drugs and dsDNA play an important role in understanding their clinical activities and the design of new targeted drugs [12]. The investigation of the interactions between prednisone and DNA is very important in terms of shedding light for further studies. Furthermore, immobilization of DNA is a key step in the biosensor construction procedure because it usually improves DNA stability. Developments in DNA biosensor production have focused on new support materials for the efficient immobilization of DNA, with many new functional materials used, such as polymer, ionic liquid, and nanoparticles [13].

Nanostructured metals have recently generated enormous interest for a wide range of technological applications because of their important size and shape-dependent features, interesting nanomorphologies, functional biocompatibility, superior electron-transfer kinetics, non-toxic features and high biological activity leading to enhanced sensing properties [14]. Among various nanostructured metals, silver nanoparticles (AgNPs) have been commonly utilized to modify the electrode surface and exhibit distinctive features such as a fast electron transfer rate, catalytic activity, good biocompatibility and low cost [15-17]. Moreover, the use of AgNPs in the manufacture of electrochemical sensors can greatly reduce the overpotential of many analytes [18, 19].

In recent years, studies on the use of electroactive polymers for sensor/biosensor development purposes have become widespread due to their electronic, optical, mechanical, conductivity and stability features [20, 21]. The main applications of conducting polymers in electrochemistry include sensors, electrocatalysis, energy storage, supercapacitors, electrochromism and electroanalysis [22-24]. Among conducting polymers, P(GBHA), which was first synthesized by our group, can be easily electropolymerized onto the GCE surface to produce a conductive thin

film with promising properties for the improvement of electrochemical sensors and biosensors [25].

In the present study, AgNPs and P(GBHA) film were electrodeposited onto a GCE by the CV technique. The dsDNA was then immobilized onto the GCE/AgNPs/P(GBHA) electrode. The effects of dsDNA concentration, dsDNA immobilization time, PRD concentration and interaction time on the electrochemical response of guanine and adenine were investigated herein. The characterization of the modified electrodes was performed by FESEM, XPS, and CV methods. In addition, the proposed biosensor has potential to be employed for the assay of PRD in serum samples and pharmaceutical formulations.

2. Experimental

2.1 Reagents and Apparatus

PRD was supplied from Sigma, with a stock solution prepared by dissolving the calculated quantity of reagent in ultra-pure water. dsDNA (fish sperm) was obtained from the Serva Company (Germany). Sodium acetate, GBHA, sodium dodecyl benzene sulfonate (SDBS), sodium chloride, and acetic acid were obtained from Sigma. Ultra-pure water was used for the preparation of 1000 μg mL^{-1} dsDNA stock solution, with the prepared solution stored at –20 °C. dsDNA solutions at more dilute concentrations were prepared by dilution of the stock solution with 0.5 mol L^{-1} ABS (pH 4.8). All other chemicals were employed without any treatment.

All electrochemical studies were realized by using Autolab PGSTAT 302N instrument combined with the FRA32M module (Eco Chemie, The Netherlands). A traditional three-electrode system was utilized with a bare/modified GCE with a diameter of 3 mm as the working electrode, a silver/silver chloride electrode (Ag/AgCl) as the reference electrode and a platinum wire as the auxiliary electrode. The experimental conditions for DPV measurements were: voltage step of 3

mV; pulse time of 0.02 s; interval time of 0.2 s; pulse amplitude of 50 mV and, scan rate of 15 mV s^{-1}. All experiments were repeated at least three times to provide reproducibility.

The surface images of bare and modified electrodes were obtained using a FEI Nova NanoSEM 650 scanning electron microscope (FEI, The Netherlands). The surface of the samples was covered with gold before the SEM images were taken. X-ray photoelectron spectroscopy (XPS) measurements were realized using a PHI 5000 Versa Probe spectrometer (Physical Electronics, USA) equipped with a monochromatic Al Kα X-ray source (hυ = 1486.6 eV). A Shimadzu UV-2550 spectrophotometer with quartz cuvettes (Shimadzu Corporation, Tokyo, Japan) was utilized for the UV–Vis absorption measurements of the samples at a wavelength range of 210-400 nm.

2.2 Fabrication of GCE/AgNPs/P(GBHA)

First, GCE was carefully polished with 0.3 µm and 0.05 µm alumina and sonicated with ethanol and ultra-pure water for 5 min. Silver nanoparticles were electrodeposited onto the GCE surface according to the literature [26]. Briefly, the AgNPs were obtained with five cycles at a scan rate of 50 mV s^{-1} in the potential range from +0.1 to –0.8 V in 0.01 mol L^{-1} H_2SO_4 solutions including 0.6 mmol L^{-1} $AgNO_3$ and 0.02 mol L^{-1} thiourea [27]. Then, the GCE/AgNPs were washed with ultra-pure water. The electrochemical synthesis and characterization of P(GBHA) has been already described in our previous study [25]. Briefly, P(GBHA) was prepared on the GC electrode by using the CV technique (potential range: (0.0) – (+1.7) V *vs*. Ag/AgCl; cycle numbers: 60; scan rate: 0.050 Vs^{-1}) in a 0.1 mol L^{-1} phosphate buffer solution (PBS, pH 7.0) including 1.0 mmol L^{-1} GBHA monomer and 0.1 mol L^{-1} SDBS.

2.3 dsDNA immobilization

The dsDNA biosensor was prepared by implementation of a potential of +0.5 V (*vs.* Ag/AgCl) for 240 s to the GCE/AgNPs/P(GBHA) electrode in 5.0 mL of 0.5 mol L^{-1} ABS (pH 4.8)

including 0.02 mol L^{-1} NaCl and 40 µg mL^{-1} of the fish sperm dsDNA at a stirring rate of 50 rpm [28]. After that, the GCE/AgNPs/P(GBHA)/dsDNA was gently washed with ABS (pH 4.8) to remove the unbounded dsDNA. Under our experimental conditions, the highest oxidation peaks for adenine and guanine were observed at +0.5 V. The adenine and guanine peaks at lower potential, such as +0.25 V, combine, resulting in the observation of a single peak. The peak currents for adenine and guanine were decreased at potentials higher than +0.5 V (this is not shown in the figure). The electrode surface at a potential of +0.5 V is positively charged, and the electrostatic attraction between the electrode surface and the negatively charged DNA molecules are probably maximum.

2.4 Interaction of PRD with dsDNA

The interaction between the PRD and the dsDNA was investigated by using the guanine and adenine oxidation peak currents as indicators. The GCE/AgNPs/P(GBHA)/dsDNA electrode was put into 0.5 mol L^{-1} ABS (pH 4.8) including different concentrations of PRD for certain times. After this treatment, the modified electrode was washed and put into PRD-free ABS before carrying out the DPV analysis.

2.5 Determination of PRD in biological samples

Human serum samples supplied from healthy volunteers were selected to study real sample analysis. PRD assays in serum samples were performed by spiking the analyte into serum samples. For this purpose, 1.0 mL PRD solution (1 mmol L^{-1}) was added to 1.0 mL serum for the analysis of PRD. DPV analysis was carried out and the regression equation of the calibration graph for the determination of PRD content in the spiked serum sample was used.

3. Results and Discussion

3.1 XPS analysis

The prepared electrodes were characterized by the XPS technique. Fig. 1 represents the survey spectra obtained for the GCE/AgNPs/P(GBHA) (a) and GCE/AgNPs/P(GBHA)/dsDNA (b). As seen in Fig. 1 (a), the presence of Ag 3d5, Ag 3d3 and Ag 3p indicates the electrodeposited AgNPs. Additionally, the appearance of Na 2p, Na 2s, S 2p, S 2s, C 1s, N 1s, Na KLL, O 1s, O KLL and Na 1s confirm the formation of the P(GBHA) polymer coating which is prepared in the presence of SDBS. After the immobilization of dsDNA onto the polymer film (Fig. 1(b)), the intensities of nitrogen and oxygen elements increased compared to the GCE/AgNPs/P(GBHA) due to the presence of the dsDNA, with the P 2p and P 2s peaks becoming apparent with DNA immobilization. [29].

3.2 SEM images

Fig. 2 shows SEM micrographs for the GCE/AgNPs, GCE/AgNPs/P(GBHA) and GCE/AgNPs/P(GBHA)/dsDNA. As shown in Fig. 2 (a), Ag electrodeposited onto the GCE consists of nanoparticles. The P(GBHA) coating on the AgNPs has a rough and compact morphology (Fig. 2(b)). The P(GBHA) film surface morphology is altered clearly due to the immobilization of dsDNA on the polymer coating (Fig. 2(c)). Energy dispersive X-ray (EDX) analysis was performed for a certain region of the modified electrodes, with the spectra presented in Fig. S1. The Ag signals demonstrate the deposition of AgNPs onto the GCE surface (Fig. S1(a)). As shown in Fig. S1(b), the C, O and N peaks clearly demonstrate the existence of the P(GBHA) coating. The P and S peaks indicate the addition of ionic phosphate species and dodecylbenzenesulfonate ions as dopants into the polymer structure, respectively. In addition, the Ag peaks indicate that the polymer film is deposited onto the AgNPs. For GCE/AgNPs/P(GBHA)/dsDNA (Fig. S1(c)), the peak intensities of the N, P and O elements increased due to the immobilization of dsDNA onto the polymer film.

3.3 Electrochemical characterization

CV was used to investigate the electrochemical characteristics of BGCE, GCE/P(GBHA), GCE/AgNPs/P(GBHA) and GCE/AgNPs/P(GBHA)/dsDNA. Fig. 3 presents a cyclic voltammogram for the BGCE and modified GCEs in 0.1 mol L^{-1} KCl with 5.0 mmol L^{-1} $Fe(CN)_6^{3-/4-}$ as a redox probe. When the GCE is covered with P(GBHA), a reduction in the separation between the peak potentials (ΔE_p) is observed, with an increase in the oxidation and reduction peak currents compared to the BGCE. It may be proposed that the positively charged P(GBHA) film both enhances the GCE surface area and electrostatically attracts the negatively charged $Fe(CN)_6^{3-/4-}$ ions [25]. At the GCE/AgNPs/P(GBHA) electrode, the peak signals of the redox probe further increased while the ΔE_p value was further reduced. The reason for this may be that silver shows a conductive character. On the other hand, the current responses of the AgNPs/P(GBHA)/dsDNA modified GCE for the redox probe are slightly higher than that of the BGCE. The results show that dsDNA is immobilized onto the GCE/AgNPs/P(GBHA) surface, and the negatively charged phosphate groups on the dsDNA modified electrode push the redox probe ions [30]. Consequently, AgNPs with good biocompatibility and high conductivity increase the current response of the electrode. The positively charged P(GBHA) layer enables successful immobilization of dsDNA by both electrostatic interaction and increasing surface area.

3.4 Optimization of dsDNA immobilization conditions

The effect of the amount of dsDNA on the immobilization process is examined via differential pulse voltammograms (DPVs) recorded for the GCE/AgNPs/P(GHBA)/dsDNA electrode. As seen in Fig. 4A, when the dsDNA concentration was increased from 1 to 50 µg mL^{-1}, the DPV peak currents for guanine and adenine increased. These peaks can be used as indicators [31, 32]. Fig. 4(B) and (C) show the dependence of the dsDNA concentration on the guanine and adenine

peak currents, respectively. The plateau for the dsDNA concentration at 40 μg mL^{-1} was caused by saturation of the dsDNA loading. Thus, 40 μg mL^{-1} of dsDNA was used for investigating the optimal amount of dsDNA.

The effect of the dsDNA immobilization time on the guanine and adenine peak currents at the GCE/AgNPs/P(GBHA) electrode was studied in the time range of 60 to 300 s. As shown in Fig. 5, the oxidation current for guanine and adenine increased with increasing time from 60 to 240 s, and, then, stabilized over 240 s. Therefore, a dsDNA immobilization time of 240 s was selected and used in further experiments.

3.5 Interaction between dsDNA and PRD

The incubation time between the dsDNA and PRD must be optimized to determine the PRD sensitively. As shown in Figure 6, when the fabricated GCE/AgNPs/P(GBHA)/dsDNA is incubated with a PRD concentration of 30 μg mL^{-1} from 30 to 210 s, the oxidation current for guanine and adenine dramatically decreased before becoming stabilized for incubation time of over 150 s. Thus, an interaction time of 150 s was adopted in this work.

The electrochemical determination of PRD was realized through use of the DPV technique at the GCE/AgNPs/P(GBHA)/dsDNA electrode. Fig. 7(A) represents the typical DPVs for dsDNA signals in the presence of 1.0 – 50.0 μg mL^{-1} PRD in 0.5 mol L^{-1} ABS (pH 4.8, 0.02 mol L^{-1} NaCl). The guanine and adenine peak current reduced with increasing the PRD concentration. To determine the PRD, the calibration curves were plotted as a function of this decrease in peak current, as shown in Fig. 7(B) and (C) for guanine and adenine, respectively. Two linear ranges were observed in the PRD concentration ranges of 1.0 – 10.0 μg mL^{-1} and 10.0 – 50.0 μg mL^{-1} depending on both the adenine and guanine bases signals. The related regression equations and determination coefficients are shown in the inset of the calibration plots. The limit of detection

(LOD) and limit of quantification (LOQ) values for PRD were determined via the following equation [33, 34]:

$$LOD = \frac{3.3s}{m}, \qquad LOQ = \frac{10s}{m} \qquad (1)$$

where *s* is the standard deviation of the current response of the lowest concentration in the linear range and *m* is the slope of the calibration curve.

The LOD and LOQ values were calculated from their first calibration curves to be 0.3 μg mL^{-1} and 0.91 μg mL^{-1} for guanine and 0.25 μg mL^{-1} and 0.76 μg mL^{-1} for adenine, respectively. Analytical characteristics of the GCE/AgNPs/P(GBHA)/dsDNA for the determination of PRD are summarized in Table 1. The within day and between day reproducibility of the developed biosensor were also investigated using the oxidation peak currents of the guanine before and after interaction with 30 μg mL^{-1} of PRD. The relative standard deviation (RSD%) values for these results were calculated and are given in Table 1. As shown in Table 1, the proposed dsDNA modified electrode exhibited excellent reproducibility for PRD determination.

The results obtained with the GCE/AgNPs/P(GBHA)/dsDNA electrode were compared to those obtained from other methods in the literature and tabulated in Table 2. It is clear that the electrochemical biosensor based on the AgNPs/P(GBHA)/dsDNA has a low detection limit and a wide linear range comparable to other methods used for the direct detection of PRD.

The nature of the interaction between small molecules and dsDNA can be explained by three models; (I) intercalative, (II) minor/major groove and (III) electrostatic bindings [37]. The binding mode between the PRD and the dsDNA can be determined by observing the shift in the guanine peak potential after the interaction. In general, the negative shifts observed in the peak potential correspond to the electrostatic binding, while the positive shifts observed in the peak potential correspond to intercalation [38, 39]. As seen from Fig. 7(A), the DPVs of the dsDNA-

PRD complex showed that there was a positive shift in the guanine peak potential with increasing PRD concentrations. Such behaviour can be ascribed to an arrangement of PRD molecules inside the dsDNA, with the formation of the dsDNA-PRD complex related to the intercalation [40]. Moreover, the reduction in the equilibrium concentration of the free dsDNA occurred due to the reduction in the oxidation signal of dsDNA. According to Eq. (2), the PRD-dsDNA complex formed between PRD and dsDNA, with this complex being electrochemically less active compared to the dsDNA. The binding constant (*K*) for the PRD-dsDNA interaction can be calculated by using Eq. 3, slightly modified according to the nature of the immobilized molecules [41-44]. Here, this equation was used because the concentration of the DNA was held constant while the concentration of prednisone changed.

$$\mathrm{dsDNA} + \mathrm{PRD} \rightleftharpoons \mathrm{PRD} - \mathrm{dsDNA} \qquad (2)$$

$$\log\left(\frac{1}{[\mathrm{PRD}]}\right) = \log K + \log\left(\frac{I_{\mathrm{PRD-dsDNA}}}{I_{\mathrm{dsDNA}} - I_{\mathrm{PRD-dsDNA}}}\right) \qquad (3)$$

where *K* shows the binding constant, I_{dsDNA} is the peak current of the dsDNA and $I_{\mathrm{PRD-dsDNA}}$ is the peak current of the PRD–dsDNA complex formed after interaction of the PRD with the dsDNA immobilized onto the GCE/AgNPs/P(GBHA) surface. The *K* value for this complex can be found from the intercept of the non-linear curve fitting plot of log(1/[PRD]) *vs.* log ($I_{\mathrm{PRD-dsDNA}}/(I_{\mathrm{dsDNA}}-I_{\mathrm{PRD-DNA}})$) (Fig. S2). The value of *K* for this interaction was calculated to be 2.8×10^{5} L mol^{-1}. This obtained *K* value is very close to that found for some intercalative binding agents [44-46].

3.6 Effect of salt concentration

To obtain more information for the binding mode between the dsDNA and PRD, the influence of NaCl concentration on the oxidation peak current of guanine was investigated by the DPV method in different ionic strength media (5.0-40.0 mmol L^{-1}) at the

GCE/AgNPs/P(GBHA)/dsDNA. If there is an electrostatic interaction between the dsDNA and the small molecule, the strength of the interaction should change dramatically with increasing NaCl concentration in the ABS [47, 48]. Fig. S3 shows that the peak current for the guanine remains nearly unaltered with increasing NaCl concentration in the ABS. It can be concluded that the electrostatic binding does not provide a significant contribution to the interaction between PRD and dsDNA.

3.7 UV-vis spectroscopy

Fig. 8 shows the UV-Vis absorption spectra obtained for a fixed concentration of dsDNA (20 mg L^{-1}) in the absence and presence of different concentrations of PRD (5 – 60 mg L^{-1}). In the absorption spectrum of free dsDNA, a peak at 260 nm was observed that results from absorption of purine and pyrimidine in DNA. As the PRD concentration added to the fixed concentration of dsDNA increases, the absorbance intensity of the dsDNA peak increased with a slight shift towards shorter wavelengths. The changes in the absorption spectrum for dsDNA can be attributed to the formation of the PRD-dsDNA complex. As seen in Table S1, the total absorption intensities of the free PRD and free dsDNA were higher than those of the dsDNA-PRD complex. These results show that there is an interaction between the PRD corticosteroid and the dsDNA. Generally, hyperchromism and hypochromism are attributed to changes in the spectral features of the DNA double stranded structure when DNA interacts with other molecules; hyperchromism refers to the fracture of the secondary structure of DNA, and hypochromism refers to the stabilization of the DNA double helix structure with small molecules through an electrostatic effect or intercalation binding mode [34, 49]. The weak hypochromism and slight blueshift mean that the interaction between PRD and dsDNA primarily occurs through intercalation. The following equation was employed to calculate the binding constant (*K*) [50]:

$$\frac{A_0}{A-A_0} = \frac{\varepsilon_G}{\varepsilon_{H-G}} + \frac{\varepsilon_G}{\varepsilon_{H-G}} \times \frac{1}{K[PDN]} \quad (4)$$

where K presents the binding constant, and A_0 and A correspond to the absorbance of the dsDNA and PRD–dsDNA complex, respectively. ε_G and ε_{H-G} are the absorption coefficient of the dsDNA and PRD–dsDNA complex, respectively. K can be estimated from the intercept-to-slope ratio of a $1/(A-A_0)$ *vs*. 1/[PRD] plot. The value of K for the interaction between PRD and dsDNA is determined to be 1.74×10^3 L mol^{-1}. This value is lower than both the value found by the DPV technique and the value for the classical intercalator ethidium bromide ($K = 1.23\times10^5$ L mol^{-1}) [51]. It can be suggested that the PRD binds to dsDNA relatively moderately under conditions in which dsDNA is not immobilized.

3.8 Interference studies

The selectivity of the developed dsDNA sensor was tested by using various biological molecules such as L-ascorbic acid, dopamine, uric acid, urea, L-cysteine, folic acid, glucose, caffeic acid, citric acid, acetylsalicylic acid, naproxen, flurbiprofen, and paracetamol. The voltammetric responses were recorded before and after adding 0.01 mmol L^{-1} of the interfering substances in 0.5 mol L^{-1} ABS (pH 4.8, 0.02 mol L^{-1} NaCl) containing 30 µg mL^{-1} PRD. The obtained DPV peak currents for the GCE/AgNPs/P(GBHA)/dsDNA are shown in Fig. S4. The signals from the interfering substances were similar to those obtained without any substances, with a relative error lower than ±9%. All these results shown that, the developed dsDNA biosensor has good selectivity for the determination of PRD.

3.9 Real sample assay

The practical applicability of the suggested method was tested with human serum samples using the GCE/AgNPs/P(GBHA)/dsDNA electrode based on a standard addition method. The serum samples were spiked with known amounts of PRD, and, then determined using the DPV

technique. The obtained results are given in Table 3. The recovery values are in the range of 97.0% and 106.4%. These high recovery values reveal that the developed biosensor has potential application to determine PRD in real samples.

Conclusion

In this work, we present for the first time a novel surface based on P(GBHA) and AgNPs modified GCE for dsDNA and PRD interaction sensing. A rapid, sensitive and selective dsDNA biosensor was developed for the determination of PRD by using the DPV method. The proposed biosensor was characterized by XPS, FESEM and electrochemical techniques. The P(GBHA) film provided an amine containing scaffold for the immobilization of dsDNA via adsorption. This led to high stability and reproducibility for the biosensor. The modified electrode showed superior analytical characteristics, such as a wide linear range (1.0-50.0 μg mL^{-1}), low detection limit (0.3 μg mL^{-1} for guanine and 0.25 μg mL^{-1} for adenine), repeatability and anti-interference ability. The results obtained from both DPV and UV-Vis spectroscopy indicated that the PRD can interact with dsDNA via mainly the intercalation binding mode. Therefore, this study is expected to supply beneficial information for a better understanding of molecular mechanisms of action and pharmacokinetics. In addition, the proposed method can make it possible to detect PRD in human serum samples with high recovery values (97.0% -106.4%). To this end, the developed sensing system is a promising candidate for detecting dsDNA-drug interaction in pharmaceutical analysis in the future.

Conflicts of interest

Authors declare no conflicts of interest.

References

[1] I. Hafström, M. Rohani, S. Deneberg, M. Wörnert, T. Jogestrand, J. Frostegård, Effects of low-dose prednisolone on endothelial function, atherosclerosis, and traditional risk factors for

atherosclerosis in patients with rheumatoid arthritis--a randomized study, The Journal of Rheumatology, 34 (2007) 1810-1816.

[2] J.F. Giddens, Concepts for Nursing Practice - E-Book, Elsevier Health Sciences, 2015.

[3] S. Wu, S. Jia, P. Xu, MicroRNA-9 as a novel prognostic biomarker in human laryngeal squamous cell carcinoma, International Journal of Clinical and Experimental Medicine, 7 (2014) 5523-5528.

[4] R. Pavlovic, L. Chiesa, S. Soncin, S. Panseri, F.T. Cannizzo, B. Biolatti, P.A. Biondi, Determination of cortisol, cortisone, prednisolone and prednisone in bovine urine by liquid chromatography–electrospray ionisation single quadrupole mass spectrometry, Journal of Liquid Chromatography & Related Technologies, 35 (2012) 444-457.

[5] A.F.C. Ruiter, N. Teeninga, J. Nauta, E. Endert, M.T. Ackermans, Determination of unbound prednisolone, prednisone and cortisol in human serum and saliva by on-line solid-phase extraction liquid chromatography tandem mass spectrometry and potential implications for drug monitoring of prednisolone and prednisone in saliva, Biomedical Chromatography, 26 (2012) 789-796.

[6] W. Guo, H. Lin, L. Liu, J. Song, Polarographic Catalytic Wave of Prednisone in the Presence of Persulfate and its Application, Microchimica Acta, 140 (2002) 97-102.

[7] R.N. Goyal, S. Bishnoi, Simultaneous voltammetric determination of prednisone and prednisolone in human body fluids, Talanta, 79 (2009) 768-774.

[8] S.K. Yadav, P. Chandra, R.N. Goyal, Y.-B. Shim, A review on determination of steroids in biological samples exploiting nanobio-electroanalytical methods, Analytica Chimica Acta, 762 (2013) 14-24.

[9] A.J.S. Ahammad, N.C.D. Nath, G.-R. Xu, S. Kim, J.-J. Lee, Interference-Free Determination of Dopamine at the Poly(thionine)-Modified Glassy Carbon Electrode, Journal of The Electrochemical Society, 158 (2011) F106-F110.

[10] G. Xu, J. Fan, K. Jiao, Studies on the Electrochemical Property of Dinuclear Copper(II) Complex Containing Dimethylglyoxime and Its Interaction with DNA, Electroanalysis, 20 (2008) 1209-1214.

[11] A. Erdem, M. Ozsoz, Electrochemical DNA Biosensors Based on DNA-Drug Interactions, Electroanalysis, 14 (2002) 965-974.

[12] L. Han, Y. Zhou, X. Huang, M. Xiao, L. Zhou, J. Zhou, A. Wang, J. Shen, A multi-spectroscopic approach to investigate the interaction of prodigiosin with ct-DNA, Spectrochimica Acta Part A: Molecular and Biomolecular Spectroscopy, 123 (2014) 497-502.

[13] K.-J. Huang, Y.-J. Liu, H.-B. Wang, Y.-Y. Wang, A sensitive electrochemical DNA biosensor based on silver nanoparticles-polydopamine@graphene composite, Electrochimica Acta, 118 (2014) 130-137.

[14] X. Wang, J. Zhuang, Q. Peng, Y. Li, A general strategy for nanocrystal synthesis, Nature, 437 (2005) 121-124.

[15] K. Cui, Y. Song, Y. Yao, Z. Huang, L. Wang, A novel hydrogen peroxide sensor based on Ag nanoparticles electrodeposited on DNA-networks modified glassy carbon electrode, Electrochemistry Communications, 10 (2008) 663-667.

[16] H. Chen, Z. Zhang, D. Cai, S. Zhang, B. Zhang, J. Tang, Z. Wu, A hydrogen peroxide sensor based on Ag nanoparticles electrodeposited on natural nano-structure attapulgite modified glassy carbon electrode, Talanta, 86 (2011) 266-270.

[17] F. Gao, T. Fan, S. Ou, J. Wu, X. Zhang, J. Luo, N. Li, Y. Yao, Y. Mou, X. Liao, D. Geng, Highly efficient electrochemical sensing platform for sensitive detection DNA methylation, and methyltransferase activity based on Ag NPs decorated carbon nanocubes, Biosensors and Bioelectronics, 99 (2018) 201-208.

[18] S. Nantaphol, O. Chailapakul, W. Siangproh, Sensitive and selective electrochemical sensor using silver nanoparticles modified glassy carbon electrode for determination of cholesterol in bovine serum, Sensors and Actuators B: Chemical, 207 (2015) 193-198.

[19] H. Wang, H. Wang, T. Li, J. Ma, K. Li, X. Zuo, Silver nanoparticles selectively deposited on graphene-colloidal carbon sphere composites and their application for hydrogen peroxide sensing, Sensors and Actuators B: Chemical, 239 (2017) 1205-1212.

[20] T.K. Das, S. Prusty, Review on Conducting Polymers and Their Applications, Polymer-Plastics Technology and Engineering, 51 (2012) 1487-1500.

[21] M.-T. Hsieh, T.-J. Whang, Mechanistic investigation on the electropolymerization of phenol red by cyclic voltammetry and the catalytic reactions toward acetaminophen and dopamine using poly(phenol red)-modified GCE, Journal of Electroanalytical Chemistry, 795 (2017) 130-140.

[22] X. Wang, T. Wang, C. Yang, H. Li, P. Liu, Well-defined flake-like polypyrrole grafted graphene nanosheets composites as electrode materials for supercapacitors with enhanced cycling stability, Applied Surface Science, 287 (2013) 242-251.

[23] M.E. Abdelhamid, A.P. O'Mullane, G.A. Snook, Storing energy in plastics: a review on conducting polymers & their role in electrochemical energy storage, RSC Advances, 5 (2015) 11611-11626.

[24] J. Janata, M. Josowicz, Conducting polymers in electronic chemical sensors, Nature Materials, 2 (2003) 19.

[25] E. Ergün, Ş. Kart, D.K. Zeybek, B. Zeybek, Simultaneous electrochemical determination of ascorbic acid and uric acid using poly(glyoxal-bis(2-hydroxyanil)) modified glassy carbon electrode, Sensors and Actuators B: Chemical, 224 (2016) 55-64.

[26] Y.-H. Chen, R. Kirankumar, C.-L. Kao, P.-Y. Chen, Electrodeposited Ag, Au, and AuAg nanoparticles on graphene oxide-modified screen-printed carbon electrodes for the voltammetric determination of free sulfide in alkaline solutions, Electrochimica Acta, 205 (2016) 124-131.

[27] G. Aydoğdu Tığ, Highly sensitive amperometric biosensor for determination of NADH and ethanol based on Au-Ag nanoparticles/poly(L-Cysteine)/reduced graphene oxide nanocomposite, Talanta, 175 (2017) 382-389.

[28] K. Pinar, K. Kagan, O. Dilsat, M. Burcu, E. Arzum, N.P. E., O. Mehmet, Label-Free and Label Based Electrochemical Detection of Hybridization by Using Methylene Blue and Peptide Nucleic Acid Probes at Chitosan Modified Carbon Paste Electrodes, Electroanalysis, 14 (2002) 1685-1690.

[29] G.A. Tığ, B. Zeybek, Ş. Pekyardımcı, Electrochemical DNA biosensor based on poly(2,6-pyridinedicarboxylic acid) modified glassy carbon electrode for the determination of anticancer drug gemcitabine, Talanta, 154 (2016) 312-321.

[30] A. Saljooqi, T. Shamspur, A. Mostafavi, Ag-4-ATP-MWCNT electrode modified with dsDNA as label-free electrochemical sensor for the detection of daunorubicin anticancer drug, Bioelectrochemistry, 118 (2017) 161-167.

[31] J. Wang, Electrochemical nucleic acid biosensors, Analytica Chimica Acta, 469 (2002) 63-71.

[32] F. Lucarelli, G. Marrazza, I. Palchetti, S. Cesaretti, M. Mascini, Coupling of an indicator-free electrochemical DNA biosensor with polymerase chain reaction for the detection of DNA sequences related to the apolipoprotein E, Analytica Chimica Acta, 469 (2002) 93-99.

[33] C.C. Chan, Analytical Method Validation: Principles and Practices, in: Pharmaceutical Sciences Encyclopedia, John Wiley & Sons, Inc., 2010.

[34] D. Koyuncu Zeybek, B. Demir, B. Zeybek, Ş. Pekyardımcı, A sensitive electrochemical DNA biosensor for antineoplastic drug 5-fluorouracil based on glassy carbon electrode modified with poly(bromocresol purple), Talanta, 144 (2015) 793-800.

[35] R.N. Goyal, S.P. Singh, S. Chatterjee, S. Bishnoi, Electrochemical investigations of prednisone using fullerene-C 60-modified edge plane pyrolytic graphite electrode, Indian Journal of Chemistry - Section A Inorganic, Physical, Theoretical and Analytical Chemistry, 49 (2010) 26-33.

[36] J.M. Gonçalves, R.R. Guimarães, B.B.N.S. Brandão, L.P.H. Saravia, P.O. Rossini, C.V. Nunes, J.S. Bernardes, M. Berttoti, L. Angnes, K. Araki, Nanostructured Alpha-NiCe Mixed Hydroxide for Highly Sensitive Amperometric Prednisone Sensors, Electrochimica Acta, 247 (2017) 30-40.

[37] R. Karimi Shervedani, H. Mirhosseini, M. Samiei Foroushani, M. Torabi, F.R. Rahsepar, L. Norouzi-Barough, Immobilization of methotrexate anticancer drug onto the graphene surface and interaction with calf thymus DNA and 4T1 cancer cells, Bioelectrochemistry, 119 (2018) 1-9.

[38] M.T. Carter, M. Rodriguez, A.J. Bard, Voltammetric studies of the interaction of metal chelates with DNA. 2. Tris-chelated complexes of cobalt(III) and iron(II) with 1,10-phenanthroline and 2,2'-bipyridine, Journal of the American Chemical Society, 111 (1989) 8901-8911.

[39] G.A. Tığ, G. Günendi, T.E. Bolelli, İ. Yalçın, Ş. Pekyardımcı, Study on interaction between the 2-(2-phenylethyl)-5-methylbenzimidazole and dsDNA using glassy carbon electrode modified with poly-3-amino-1,2,4-triazole-5-thiol, Journal of Electroanalytical Chemistry, 776 (2016) 9-17.

[40] K. Nemčeková, J. Labuda, V. Milata, J. Blaškovičová, J. Sochr, Interaction of DNA and mononucleotides with theophylline investigated using electrochemical biosensors and biosensing, Bioelectrochemistry, 123 (2018) 182-189.

[41] M.S. Ibrahim, Voltammetric studies of the interaction of nogalamycin antitumor drug with DNA, Analytica Chimica Acta, 443 (2001) 63-72.

[42] H. Nawaz, S. Rauf, K. Akhtar, A.M. Khalid, Electrochemical DNA biosensor for the study of ciprofloxacin–DNA interaction, Analytical Biochemistry, 354 (2006) 28-34.

[43] B. Rafique, A.M. Khalid, K. Akhtar, A. Jabbar, Interaction of anticancer drug methotrexate with DNA analyzed by electrochemical and spectroscopic methods, Biosensors and Bioelectronics, 44 (2013) 21-26.

[44] G. Aydoğdu, G. Günendi, D.K. Zeybek, B. Zeybek, Ş. Pekyardımcı, A novel electrochemical DNA biosensor based on poly-(5-amino-2-mercapto-1,3,4-thiadiazole) modified glassy carbon electrode for the determination of nitrofurantoin, Sensors and Actuators B: Chemical, 197 (2014) 211-219.

[45] B. Dogan-Topal, B. Bozal-Palabiyik, S.A. Ozkan, B. Uslu, Investigation of anticancer drug lapatinib and its interaction with dsDNA by electrochemical and spectroscopic techniques, Sensors and Actuators B: Chemical, 194 (2014) 185-194.

[46] M. Sirajuddin, S. Ali, A. Badshah, Drug–DNA interactions and their study by UV–Visible, fluorescence spectroscopies and cyclic voltametry, Journal of Photochemistry and Photobiology B: Biology, 124 (2013) 1-19.

[47] J.-H. Shi, J. Chen, J. Wang, Y.-Y. Zhu, Binding interaction between sorafenib and calf thymus DNA: Spectroscopic methodology, viscosity measurement and molecular docking, Spectrochimica Acta Part A: Molecular and Biomolecular Spectroscopy, 136 (2015) 443-450.

[48] L. Strekowski, B. Wilson, Noncovalent interactions with DNA: An overview, Mutation Research/Fundamental and Molecular Mechanisms of Mutagenesis, 623 (2007) 3-13.

[49] M. Rahban, A. Divsalar, A.A. Saboury, A. Golestani, Nanotoxicity and Spectroscopy Studies of Silver Nanoparticle: Calf Thymus DNA and K562 as Targets, The Journal of Physical Chemistry C, 114 (2010) 5798-5803.

[50] C.D. Kanakis, P.A. Tarantilis, H.-A. Tajmir-Riahi, M.G. Polissiou, DNA Interaction with Saffron's Secondary Metabolites Safranal, Crocetin, and Dimethylcrocetin, DNA and Cell Biology, 26 (2007) 63-70.

[51] A. Dimitrakopoulou, C. Dendrinou-Samara, A.A. Pantazaki, M. Alexiou, E. Nordlander, D.P. Kessissoglou, Synthesis, structure and interactions with DNA of novel tetranuclear, [Mn4(II/II/II/IV)] mixed valence complexes, Journal of Inorganic Biochemistry, 102 (2008) 618-628.

Fig. 1 XPS survey spectra of (a) GCE/AgNPs/P(GBHA) (blue curve) and (b) GCE/AgNPs/P(GBHA)/dsDNA (red curve) electrode.

Fig. 2 SEM images of (a) GCE/AgNPs, (b) GCE/AgNPs/P(GBHA) and (c) GCE/AgNPs/P(GBHA)/dsDNA electrode.

Fig. 3 Cyclic voltammograms of (a) BGCE (black curve), (b) GCE/P(GBHA) (blue curve), (c) GCE/AgNPs/P(GBHA) (red curve) and, (d) GCE/Ag/P(GBHA)/dsDNA (orange

curve) electrodes at scan rate 50 mVs^{-1} in 1.0 mol L^{-1} KCl solution containing 5 mmol L^{-1} $Fe(CN)_6^{3-/4-}$.

Fig. 4 (A) Differential pulse voltammogram of the GCE/AgNPs/P(GBHA) electrode at dsDNA amounts varying from 5.0 μg mL^{-1} (black curve) to 60.0 μg mL^{-1} (purple curve) μg mL^{-1}. The effect of dsDNA concentration on the electrochemical responses of (B) guanine and (C) adenine at GCE/AgNPs/P(GBHA)/dsDNA.

Fig. 5 The effect of dsDNA immobilization time on the electrochemical responses of guanine (black block) and adenine (red block) at GCE/AgNPs/P(GBHA)/dsDNA.

Fig. 6 The effect of the interaction time of PRD with dsDNA on the guanine (black block) and adenine (red block) oxidation peak currents (0.5 mol L^{-1} ABS, pH 4.8).

Fig. 7 (A) Differential pulse voltammograms of the interaction of PRD with the dsDNA at GCE/AgNPs/P(GBHA)/dsDNA. The oxidation signals of guanine and adenine after interaction with different concentrations of PRD amounts varying from 1.0 μg mL^{-1} (black curve) to 50.0 μg mL^{-1} (purple curve); linear dependence of PRD concentration on the (B) guanine and (C) adenine signals at GCE/AgNPs/P(GBHA)/dsDNA electrode. The regression equations of guanine: y = -0.08x + 1.60 (R^2=0.980) for the first line and y = -0.012x + 0.94 (R^2=0.990) for the second line. The regression equations of adenine: y = -0.15x + 2.71 (R^2=0.991) for the first line and y = -0.023x + 1.46 (R^2=0.998) for the second line.

Fig. 8 UV-vis absorption spectra of dsDNA (30 μg mL^{-1}) in the absence (black curve) and presence of the PRD in the range of 5.0 μg mL^{-1} (red curve) – 60 μg mL^{-1} (purple curve).

Table 1 Analytical characteristics of the GCE/AgNPs/P(GBHA)/dsDNA for the determination of PRD*

Parameters	**Results (guanine)**	**Results (adenine)**
Linearity range (μg mL^{-1})	1.0-10.0 (1) 10.0-50.0 (2)	1.0-10.0 (1) 10.0-50.0 (2)
Slope (μA μg^{-1} mL)	0.08 (1) 0.012 (2)	0.15 (1) 0.023 (2)
Intercept (μA)	1.60 (1) 0.94 (2)	2.71 (1) 1.46 (2)
SE of slope (μA μg^{-1} mL)	0.006 (1) 5.95×10^{-4} (2)	0.008 (1) 5.14×10^{-4} (2)
SE of intercept (μA)	0.041 (1) 0.015 (2)	0.052 (1) 0.0184 (2)
Determination coefficient	0.980 (1) 0.990 (2)	0.991 (2) 0.998 (2)
LOD (μg mL^{-1})	0.30	0.25
LOQ (μg mL^{-1})	0.91	0.76
Within day reproducibility (RSD%)	1.16	1.24
Between day reproducibility (RSD%)	1.08	0.94

*The results were given average of five measurements.

Table 2 Comparison of analytical performances of the different electrochemical sensors for the determination of PRD.

Electrode	Linearity	LOD	Reproducibility	Application	Reference
SWNT/EPPGE	0.01 – 100 μmol L^{-1}	0.45×10^{-8} mol L^{-1}	RSD: 3.24%	Plasma Recoveries:96.60–103.28	[7]
C_{60}/EPPGE	5.0×10^{-8}–5.0×10^{-5} mol L^{-1}	4.8×10^{-8} mol L^{-1}	RSD: 0.94% (n=6)	Plasma Recoveries:97.44–103.50 Urine Recoveries:97.20–103.12	[35]
α-NiCe/FTO (Amperometric)	0.5–76.9×10^{-6} mol L^{-1}	4.8×10^{-8} mol L^{-1}	NA	NA	[36]
α-NiCe/FTO (FIA)	4.0–10.0×10^{-6} mol L^{-1}	0.84×10^{-8} mol L^{-1}	NA	NA	[36]
GCE/AgNPs/P(GBHA)/dsDNA	1.0−50.0 μg mL^{-1}	0.3 μg mL^{-1} (8.37×10^{-7} mol L^{-1}) for guanine, 0.25 μg mL^{-1} (6.97×10^{-7} mol L^{-1}) for adenine	RSD: 1.16% for guanine, 1.245 for adenine (n=5)	Serum Recoveries: 97.0–106.4	This study

Single wall carbon nanotube (SWNT), edge plane pyrolytic graphite electrode (EPPGE), fullerene C_{60} (C_{60}), glassy carbon electrode (GCE), silver nanoparticles (AgNPs), poly(glyoxal-bis(2-hydroxyanil)) (P(GBHA)), double stranded DNA (dsDNA), relative standard deviation (RSD). NA: Not Applicable

Table 3 Determination of PRD in human serum samples.

Sample no	Amount of added ($\mu g\ mL^{-1}$)	Amount of found ($\mu g\ mL^{-1}$)	RSD (%)	Recovery (%)
1	1.0	0.97	0.88	97.0
2	5.0	5.32	1.24	106.4
3	10.0	10.16	1.92	101.6
4	25.0	26.08	1.37	104.32

Highlights

- Ag nanoparticles and poly(glyoxal-bis(2-hydroxyanil)) film were deposited on a GCE
- DNA biosensor was prepared by immobilization of dsDNA onto the modified GCE
- Interaction between prednisone (PRD) and dsDNA was examined by using DPV and UV-VIS
- The fabricated biosensor has a wide linear response range of 1.0−50 μg mL^{-1} for PRD

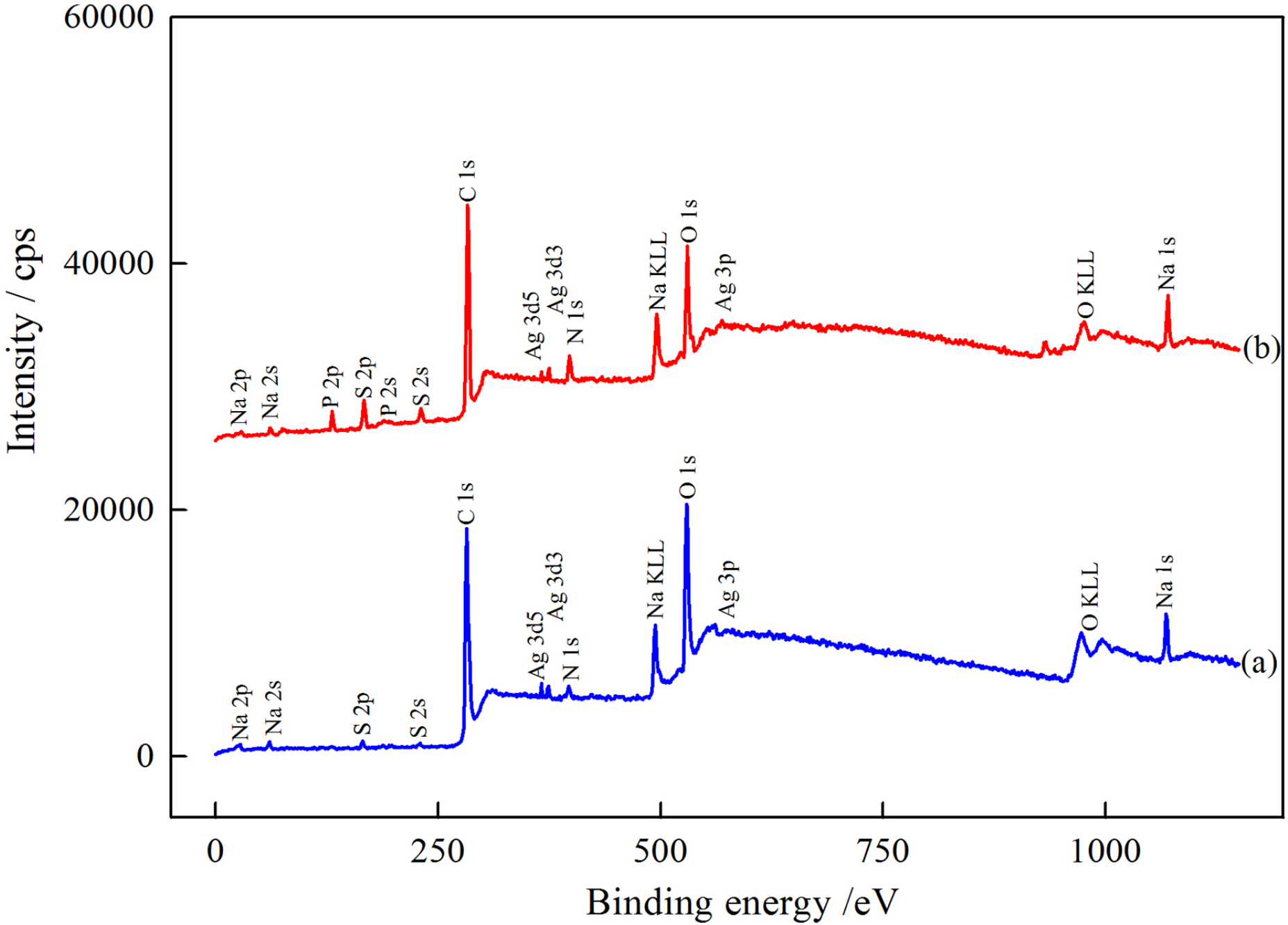
60000
40000
20000
0
Intensity / cps
0
250
500
750
1000
Binding energy /eV
Na 2p
Na 2s
P 2p
S 2p
P 2s
S 2s
C 1s
Ag 3d5
Ag 3d3
N 1s
Na KLL
O 1s
Ag 3p
O KLL
Na 1s
(b)
(a)

Figure 1

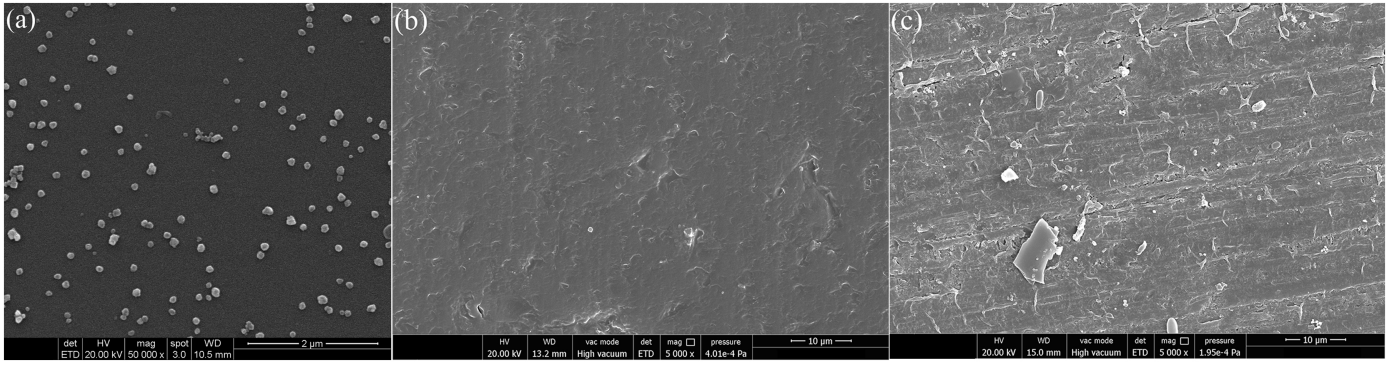
(a)
det ETD
HV 20.00 kV
mag 50 000 x
spot 3.0
WD 10.5 mm
2 µm
(b)
HV 20.00 kV
WD 13.2 mm
vac mode High vacuum
det ETD
mag 5 000 x
pressure 4.01e-4 Pa
10 µm
(c)
HV 20.00 kV
WD 15.0 mm
vac mode High vacuum
det ETD
mag 5 000 x
pressure 1.95e-4 Pa
10 µm

Figure 2

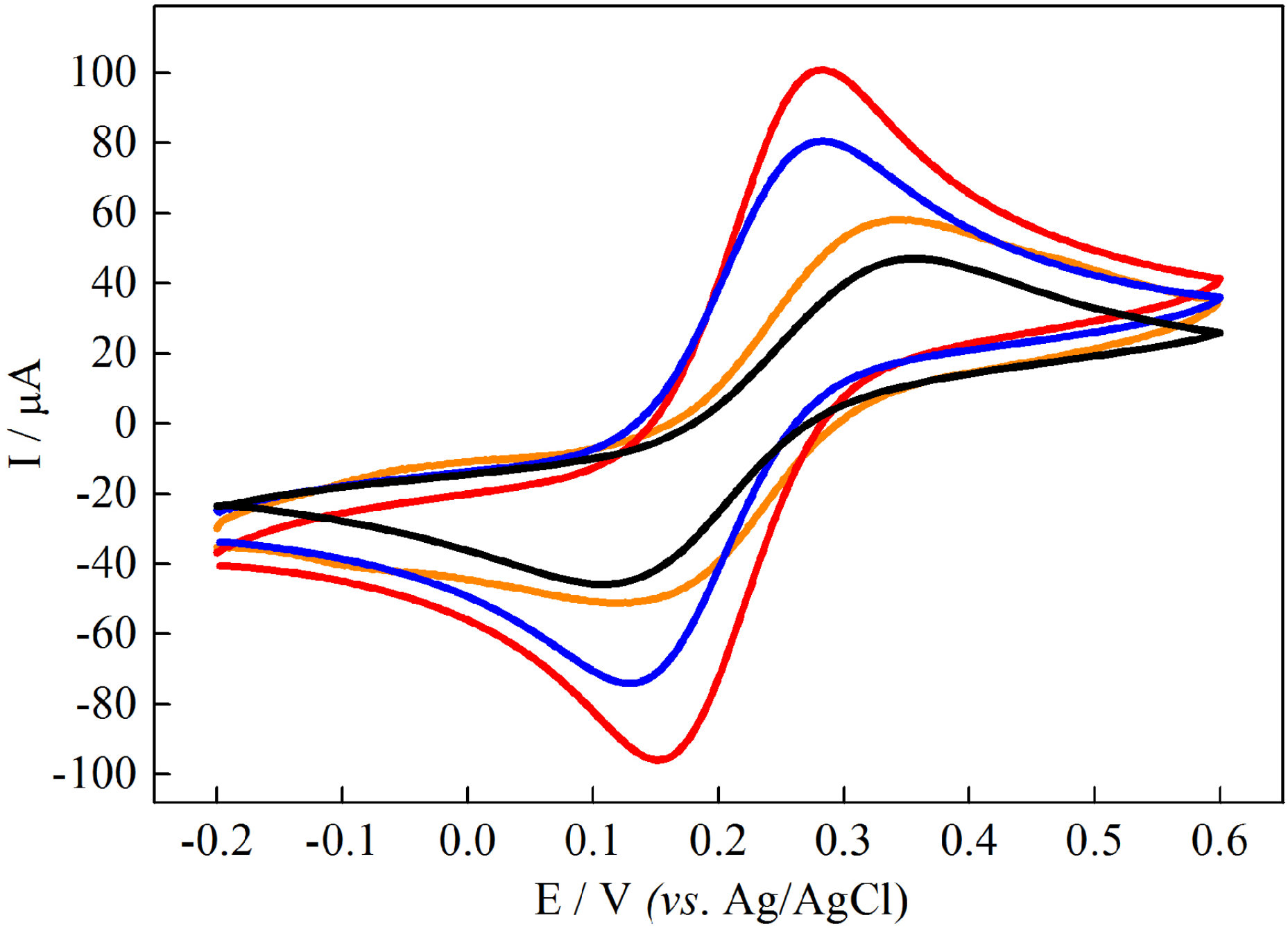
100
80
60
40
20
0
-20
-40
-60
-80
-100
I / μA
-0.2
-0.1
0.0
0.1
0.2
0.3
0.4
0.5
0.6
E / V (vs. Ag/AgCl)

Figure 3

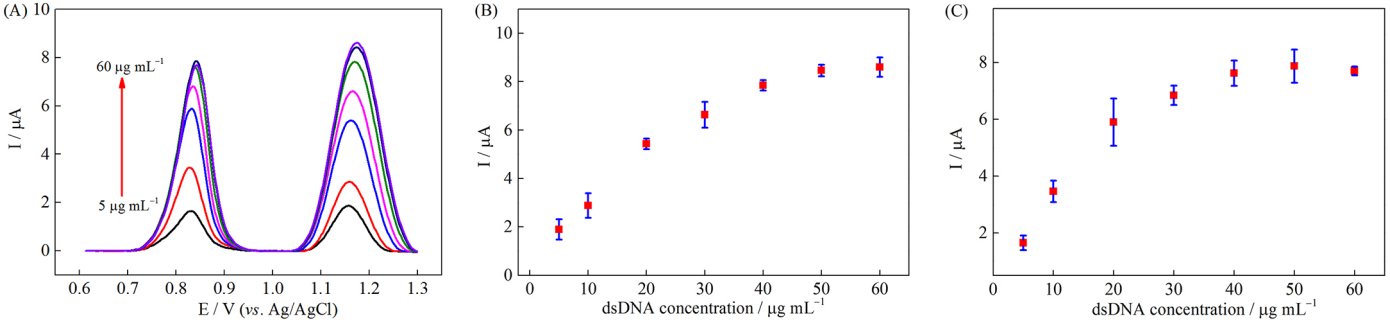
(A)
60 μg mL⁻¹
5 μg mL⁻¹
I / μA
E / V (vs. Ag/AgCl)
(B)
I / μA
dsDNA concentration / μg mL⁻¹
(C)
I / μA
dsDNA concentration / μg mL⁻¹

Figure 4

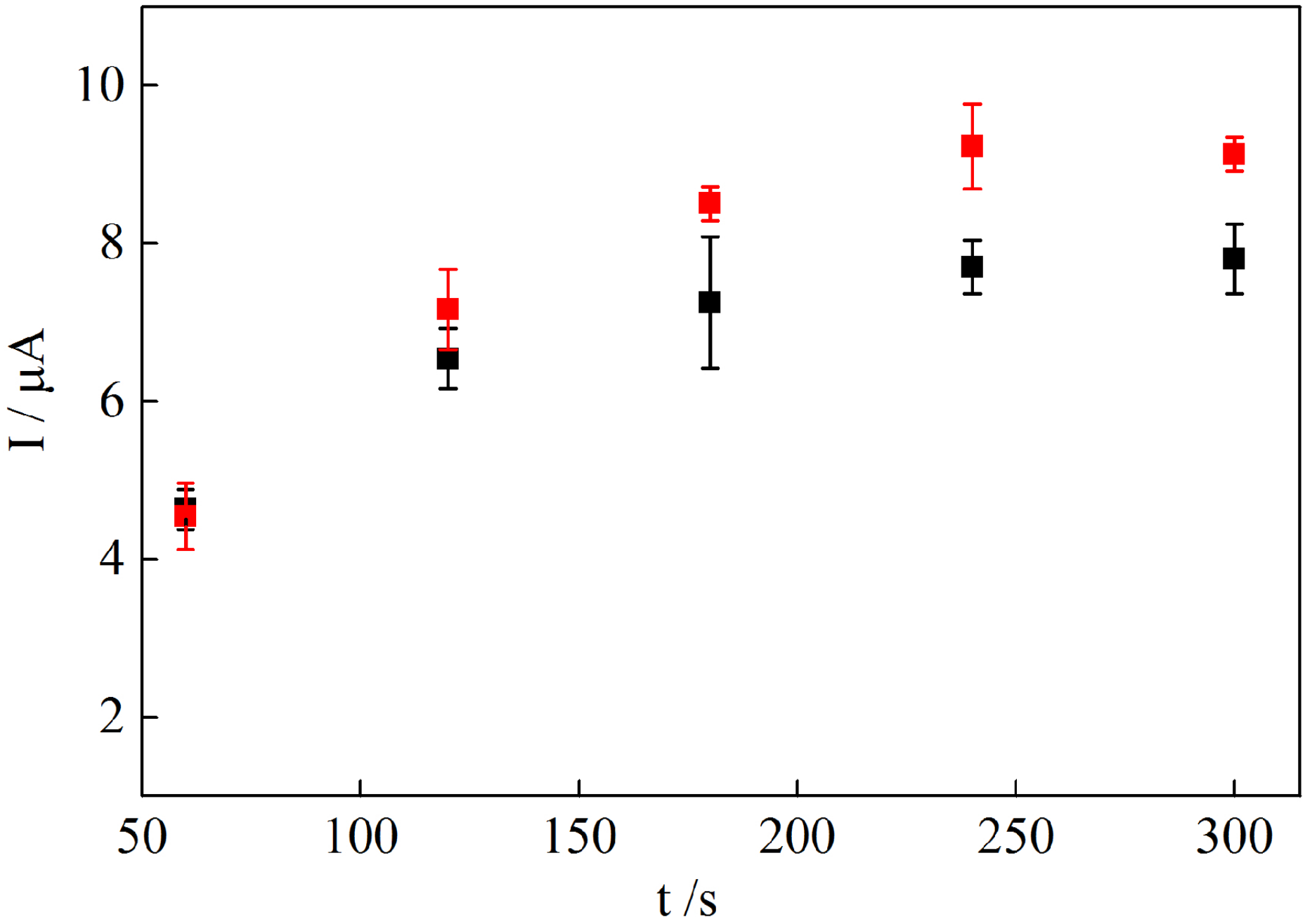

Figure 5

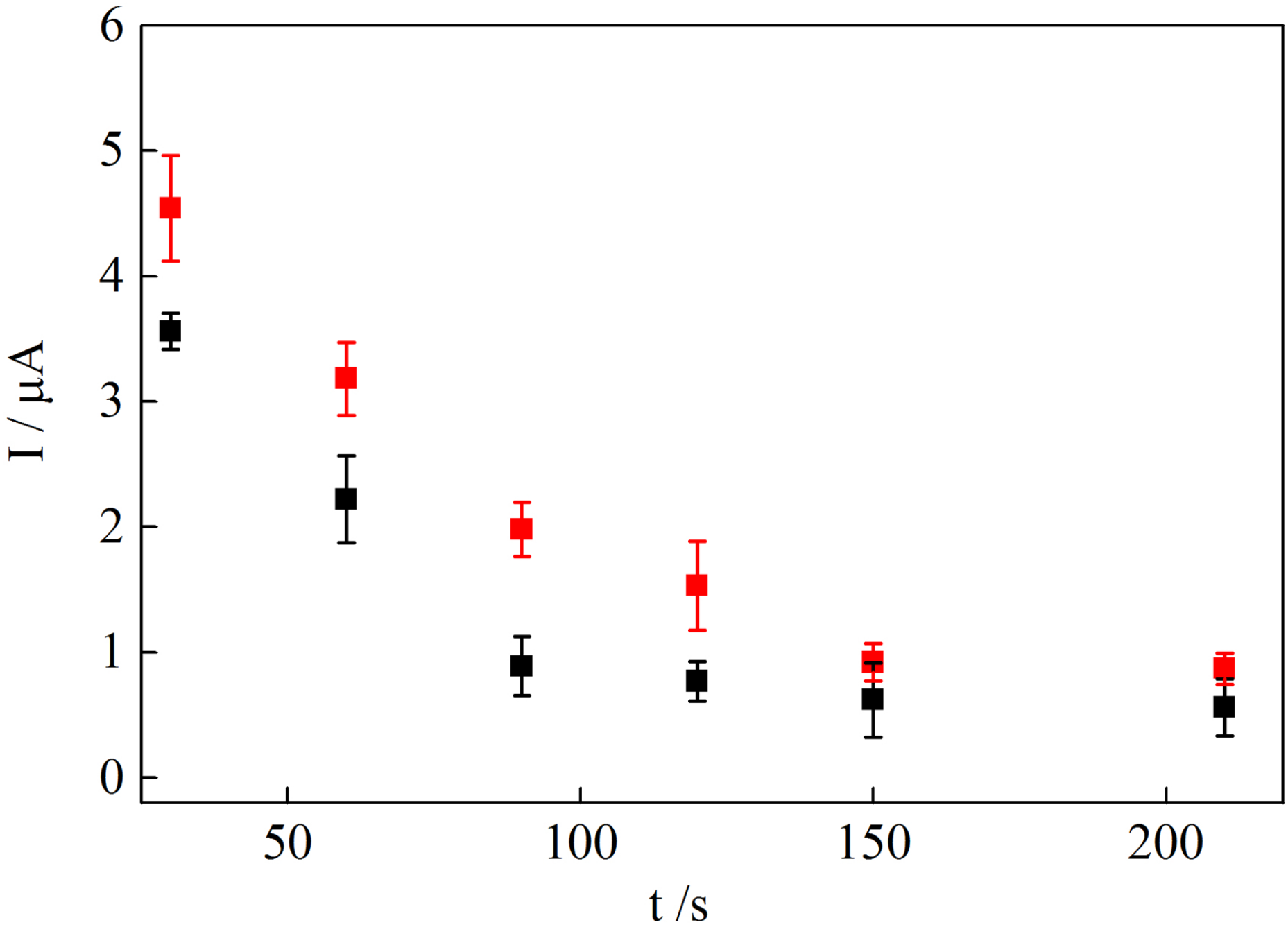

Figure 6

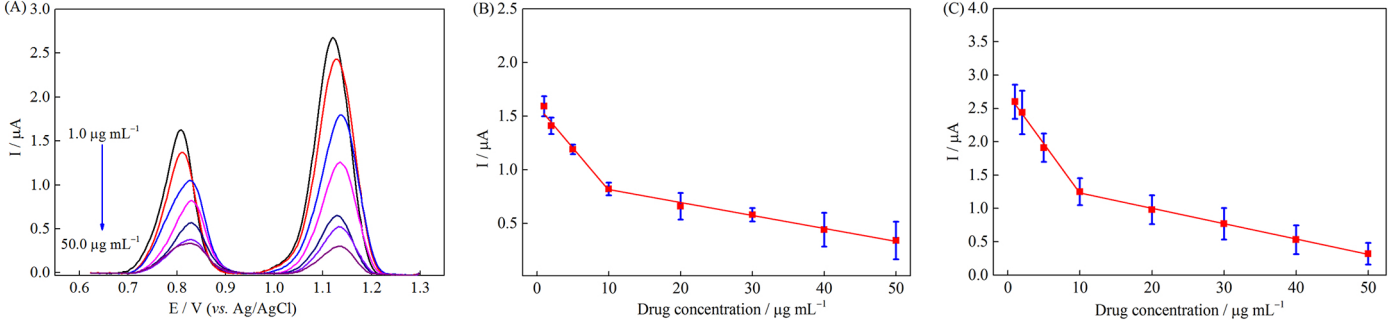
(A)
I / μA
1.0 μg mL⁻¹
50.0 μg mL⁻¹
E / V (vs. Ag/AgCl)
(B)
I / μA
Drug concentration / μg mL⁻¹
(C)
I / μA
Drug concentration / μg mL⁻¹

Figure 7

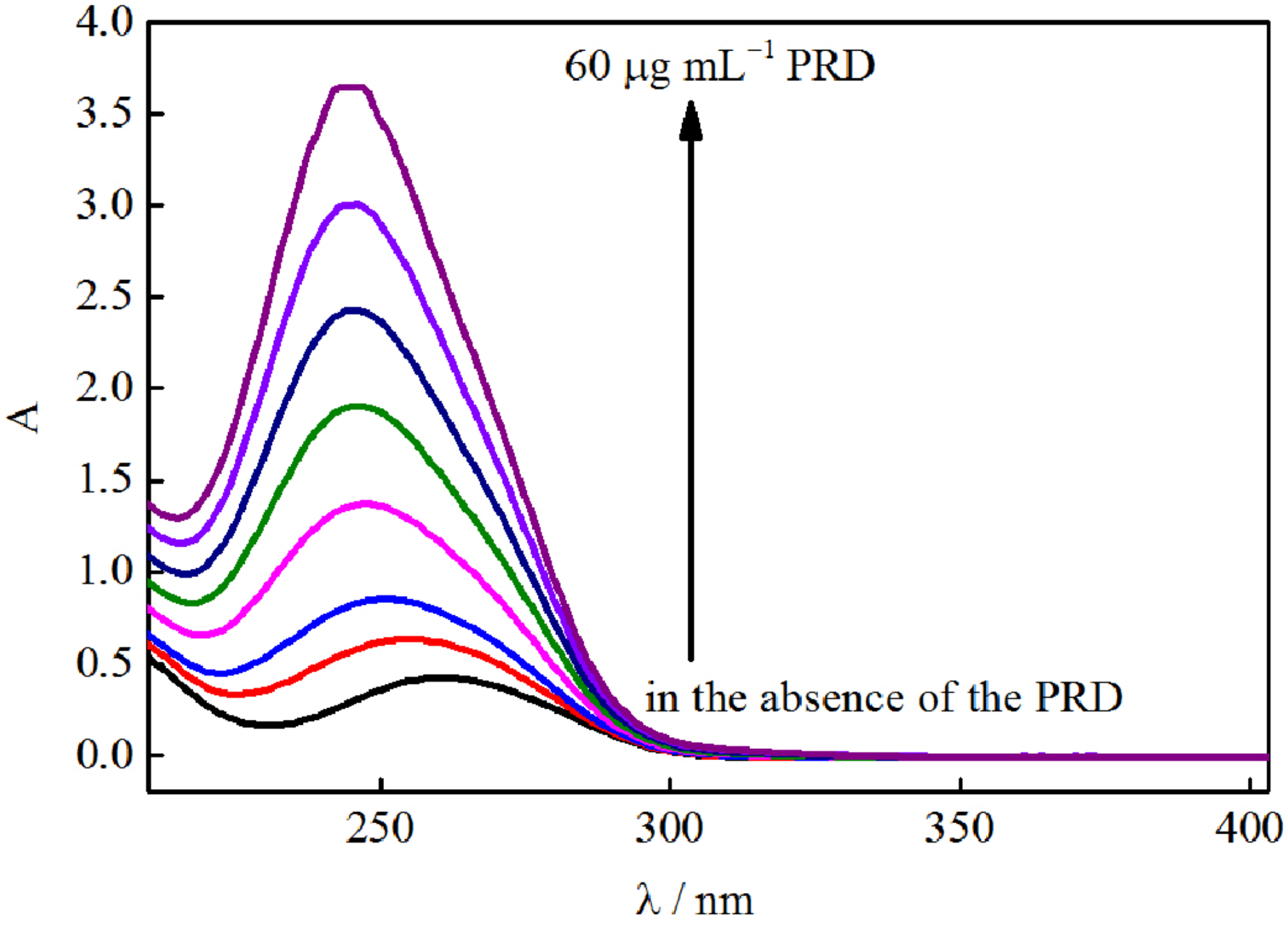
4.0
3.5
3.0
2.5
2.0
1.5
1.0
0.5
0.0
A
60 μg mL^{-1} PRD
in the absence of the PRD
250
300
350
400
λ / nm

Figure 8